Human-Exoskeleton Multibody System Dynamics to Study Assistance During Standing and Walking Tasks

Keaton Inkol and John McPhee

May 30, 2024

Human-Exoskeleton Multibody System Dynamics to Study Assistance During Standing and Walking Tasks

Keaton A. Inkol, John McPhee

Systems Design Engineering
University of Waterloo, Waterloo, Canada
kainkol@uwaterloo.ca, mcphee@uwaterloo.ca

Abstract

In the past decade, powered robotic lower-limb exoskeletons have emerged as an exciting technological advancement, offering enhancements in mobility and quality of life for individuals with physical impairments. Addressing deficits in human mobility is a challenge, given the multitude of conditions that can impact a person's ability to move [5]. To address these challenges, researchers have begun investigating model-based assistive control; however, one must obtain a reliable model with which human-exoskeleton motions can be simulated [2]. The current abstract presents a generalized multibody dynamic model of a human wearing a lower-limb exoskeleton with early applications based on proof-of-concept simulations.

To begin, sagittal floating-base generalized coordinates pertaining to the human ($\mathbf{q}_{\mathrm{h}} \in \mathbb{R}^{q_{\mathrm{h}}}$) and exoskeleton ($\mathbf{q}_{\mathrm{e}} \in \mathbb{R}^{q_{\mathrm{e}}}$) are specified [1], i.e., joint angles combined with translations/rotations of the pelvis segment. Evolution of these coordinates are subject to second-order ODEs:

$$\begin{bmatrix} \mathbf{M}_{\mathrm{h}} & \mathbf{0} \\ \mathbf{0} & \mathbf{M}_{\mathrm{e}} \end{bmatrix} \begin{Bmatrix} \ddot{\mathbf{q}}_{\mathrm{h}} \\ \ddot{\mathbf{q}}_{\mathrm{e}} \end{Bmatrix} = \begin{Bmatrix} \mathbf{\Gamma}_{\mathrm{h}} + \boldsymbol{\tau}_{\mathrm{mtg}} \\ \mathbf{\Gamma}_{\mathrm{e}} + \boldsymbol{\tau}_{\mathrm{ac}} \end{Bmatrix} + \begin{bmatrix} \mathbf{J}_{\mathrm{he}}^{\mathsf{T}} & \mathbf{J}_{\mathrm{env}}^{\mathsf{T}} \end{bmatrix} \begin{Bmatrix} \mathbf{F}_{\mathrm{he}} \\ \mathbf{F}_{\mathrm{env}} \end{Bmatrix} \tag{1}$$

where $\mathbf{M}_{\mathrm{h}} \in \mathbb{R}^{q_{\mathrm{h}} \times q_{\mathrm{h}}}$ and $\mathbf{M}_{\mathrm{e}} \in \mathbb{R}^{q_{\mathrm{e}} \times q_{\mathrm{e}}}$ are the symmetric configuration-dependent inertia matrices and $\mathbf{\Gamma}_{\mathrm{h}} : \mathbb{R}^{q_{\mathrm{h}}} \times T_{\mathbf{q}}\mathbb{R}^{q_{\mathrm{h}}} \to \mathbb{R}^{q_{\mathrm{h}} \times 1}$ and $\mathbf{\Gamma}_{\mathrm{e}} : \mathbb{R}^{q_{\mathrm{e}}} \times T_{\mathbf{q}}\mathbb{R}^{q_{\mathrm{e}}} \to \mathbb{R}^{q_{\mathrm{e}} \times 1}$ are functions that map generalized positions/velocities to gravitational potential torques/forces and centrifugal/coriolis terms. The device itself is actuated via $\boldsymbol{\tau}_{\mathrm{ac}}$ which contains torques arising from motors, gearing friction, etc. [4]. The human component of the model is actuated via nonlinear muscle torque generators (MTGs), which allow for biofidelic human motion predictions without requiring complex musculoskeletal geometry and redundant musculature [4, 6]. Mathematically, the MTGs are expressed as

$$\boldsymbol{\tau}_{\mathrm{mtg}}(\mathbf{q}_{\mathrm{h}}(t), \dot{\mathbf{q}}_{\mathrm{h}}, \mathbf{a}^{\mathrm{fx}}(t), \mathbf{a}^{\mathrm{ex}}(t)) = \mathbf{a}^{\mathrm{fx}}(t)\boldsymbol{\tau}_{\mathrm{iso}}^{\mathrm{fx}}\boldsymbol{\tau}_{\theta}(\mathbf{q}_{\mathrm{h}})\boldsymbol{\tau}_{\omega}(\dot{\mathbf{q}}_{\mathrm{h}}) + \mathbf{a}^{\mathrm{ex}}(t)\boldsymbol{\tau}_{\mathrm{iso}}^{\mathrm{ex}}\boldsymbol{\tau}_{\theta}(\mathbf{q}_{\mathrm{h}})\boldsymbol{\tau}_{\omega}(\dot{\mathbf{q}}_{\mathrm{h}}) + \boldsymbol{\tau}_{\mathrm{psv}}(\mathbf{q}_{\mathrm{h}}, \dot{\mathbf{q}}_{\mathrm{h}}) \tag{2}$$

where $\mathbf{a}^{\mathrm{fx}}$ and $\mathbf{a}^{\mathrm{ex}}$ are flexor and extensor neural MTG activations ($a_i \in [0,1]$), while $\boldsymbol{\tau}_{\mathrm{iso}}^{\mathrm{fx}}$ and $\boldsymbol{\tau}_{\mathrm{iso}}^{\mathrm{ex}}$ are isometric torque parameter column matrices that determine peak MTG output at zero joint-velocity and the optimal joint angle. The final component in Equation (2) are the position ($\boldsymbol{\tau}_{\theta}$) and velocity scaling functions ($\boldsymbol{\tau}_{\omega}$) that allow MTGs to behave like Hill-type muscles at varying locations in state-space [6].

A major component of these integrated multibody dynamic systems, is how we define the physical interactions between the human, device and environment, i.e., how to solve for interaction forces/torques $\mathbf{F}_{\mathrm{he}}$ and $\mathbf{F}_{\mathrm{env}}$. Most frequently, we assume that these interactions are rigid in nature and can be modelled through the use of kinematic constraint equations. By defining these constraints, we can treat constraining forces/torques $\mathbf{F}_{\mathrm{he}}$ and $\mathbf{F}_{\mathrm{env}}$ as Lagrange multipliers. In the same capacity, if we assume that any changes in contact between human-exoskeleton and the environment are plastic in nature, we can then define reset maps for the generalized positions and velocities from impulse-momentum theorem [1], i.e.,

$$\mathbf{q}_{\mathrm{h}}^{+} = \mathbf{q}_{\mathrm{h}}^{-}, \quad \mathbf{q}_{\mathrm{e}}^{+} = \mathbf{q}_{\mathrm{e}}^{-} \tag{3}$$

$$\begin{Bmatrix} \dot{\mathbf{q}}_{\mathrm{h}}^{+} \\ \dot{\mathbf{q}}_{\mathrm{e}}^{+} \end{Bmatrix} = \begin{Bmatrix} \dot{\mathbf{q}}_{\mathrm{h}}^{-} \\ \dot{\mathbf{q}}_{\mathrm{e}}^{-} \end{Bmatrix} + \begin{bmatrix} \mathbf{M}_{\mathrm{h}} & \mathbf{0} \\ \mathbf{0} & \mathbf{M}_{\mathrm{e}} \end{bmatrix}^{-1} \begin{bmatrix} \mathbf{J}_{\mathrm{he}}^{\mathsf{T}} & \mathbf{J}_{\mathrm{env}}^{\mathsf{T}} \end{bmatrix} \begin{Bmatrix} \boldsymbol{\delta}_{\mathrm{he}} \\ \boldsymbol{\delta}_{\mathrm{env}} \end{Bmatrix} \tag{4}$$

where the notation x^{+} and x^{-} indicates $x(t)$ at the instant after and prior to impact while $\boldsymbol{\delta}$ represents impulses that occur from the introduction of new constraints to the unconstrained system dynamics.

To highlight how such a model can be used, we have produced simulation studies of human-exoskeleton feet-in-place balance control [4]. In Fig. 1, we assess how users of different muscle strength levels may interact with novel model-based feedback assistance during balancing. For users with 40% and 70% of baseline young adult muscle strength, their capacity to balance is reduced [7]; however, we can see that novel feedback control with a user of this strength helps with stabilization of the whole-body

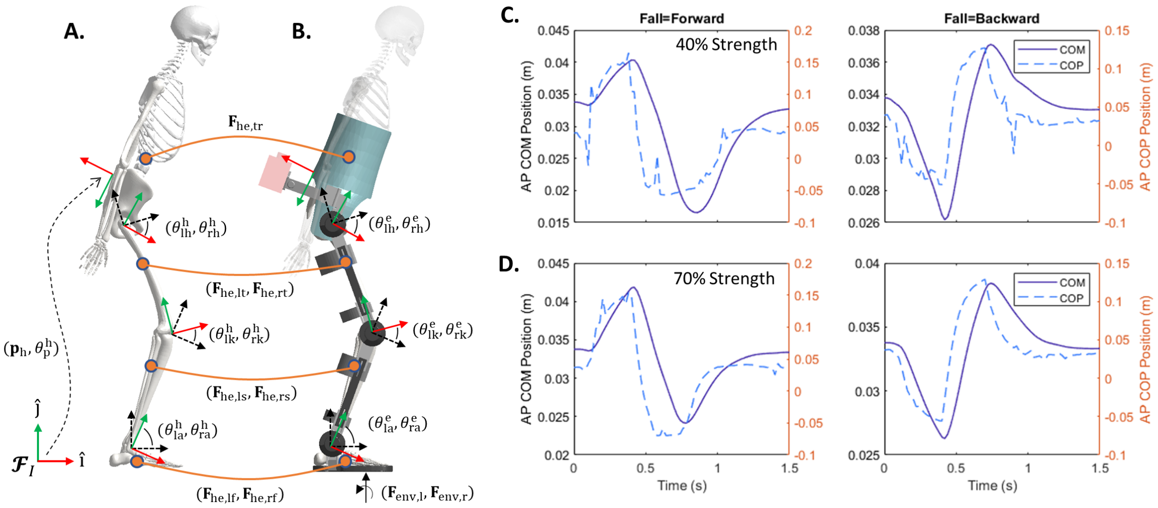

Figure 1: **A**. Floating-base human and **B**. lower-limb exoskeleton models (based on the Technaid EXO-H3). Note: the human is shown transparently in **B** to highlight how the exoskeleton fits the user. Orange circles/lines highlight where the exoskeleton was rigidly fixed to the human by reaction forces $\mathbf{F}_{\mathrm{he}}$, while $\mathbf{F}_{\mathrm{env}}$ includes right/left foot-ground reaction forces applied to the exoskeleton. Also, anteroposterior (AP) COM/COP trajectories obtained via model-based feedback control paired with nonlinear state estimation to assist a simulated **C**. 40%-strength and **D**. 70%-strength end-user with feet-in-place balance. recovery.

center of mass (COM) within the support polygon. We also observe regulation of the center of pressure (COP) within that same polygon, suggesting that the feet stayed in place during corrective maneuvers. This occurred despite both the simulated human and device having no knowledge of each other's actions.

We should note that the formulation of this model makes it suitable for a wide range of sagittal plane motor tasks, e.g., walking, standing, and sit-to-stand. Future directions should focus on the development and validation of compliant human-exoskeleton interactions and exoskeleton/human-environment interactions; to date, we have begun investigating the complex nature of compliant human-exoskeleton interactions [3]. Likewise, future developments will extend the model derivation to capture 3D phenomena.

References

[1] J. W. Grizzle, C. Chevallereau, R. W. Sinnet, and A. D. Ames. Models, feedback control, and open problems of 3D bipedal robotic walking. *Automatica*, 50(8):1955–1988, 2014.

[2] T. Gurriet et al. Towards Restoring Locomotion for Paraplegics: Realizing Dynamically Stable Walking on Exoskeletons. In *2018 IEEE International Conference on Robotics and Automation (ICRA)*, pages 2804–2811, Brisbane, 2018. IEEE.

[3] K. A. Inkol and J. McPhee. Towards compliant human-exoskeleton interactions within dynamics multibody simulations of assisted human motor control. In *10th ECCOMAS Thematic Conference on Multibody Dynamics 2021*, Budapest, Hungary, 2021.

[4] K. A. Inkol and J. McPhee. Using Dynamic Simulations to Estimate the Feasible Stability Region of Feet-In-Place Balance Recovery for Lower-Limb Exoskeleton Users. In *9th IEEE RAS/EMBS International Conference for Biomedical Robotics and Biomechatronics (BioRob)*, pages 1–6, Seoul, Korea, 2022. IEEE.

[5] Y. W. Ju, J. S. Lee, Y.-A. Choi, and Y. H. Kim. Causes and Trends of Disabilities in Community-Dwelling Stroke Survivors: A Population-Based Study. *Brain Neurorehabil*, 15(1):e5, 2022.

[6] M. Millard, A. L. Emonds, M. Harant, and K. Mombaur. A reduced muscle model and planar musculoskeletal model fit for the simulation of whole-body movements. *J Biomech*, 89:11–20, 2019.

[7] Y. C. Pai and J. Patton. Center of mass velocity-position predictions for balance control. *J Biomech*, 30(4):347–354, 1997.